The Journal of Green Energy and Environmental Engineering

Research Paper

Synthesis of Nitrogen-Phosphorus Flame Retardant and Its Flame-Retardant Application in Epoxy Resin

William Chen[1], Emma Nilsson[1,*], Isabella Santos[2]

[1] Center for Microtechnologies, University of Wollongong, Wollongong, Australia
[2] Faculty of Light Engineering, University of Reading, United Kingdom
*Corresponding author: drgchen@gmail.com; Nilsson98@gmail.com; Santos_since2020@henley.ac.uk

Abstract. A novel multielement synergistic flame retardant (DAI) was successfully synthesized via a two-step reaction using 9,10-dihydro-9-oxa-10-phosphaphenanthrene-10-oxide (DOPO), 2-aminobenzothiazole (ABZ), and indole-3-carboxaldehyde (I3C). The successful synthesis of DAI was confirmed by Fourier transform infrared spectroscopy (FT-IR) and nuclear magnetic resonance (NMR) spectroscopy. Subsequently, epoxy resin (EP) composites, namely EP/DAI-3, EP/DAI-5, and EP/DAI-7, were prepared by blending DAI with EP via a thermosetting method. The flame-retardant properties and residual char characteristics after combustion of the prepared EP composites were investigated. The results demonstrated that the prepared EP composites exhibited excellent smoke suppression and flame-retardant performance. Particularly, EP incorporating 7 wt% DAI showed significant reductions of 34.5%, 32.3%, and 42.2% in peak heat release rate (pHRR), peak CO production rate (pCOPR), and peak CO_2 production rate (pCO_2PR), respectively. Compared with pure EP, EP/DAI-7 achieved a limiting oxygen index (LOI) value of 32.6% and attained a V-0 rating in the UL-94 test. Char residue analysis revealed that the char layer of EP/DAI-7 was denser and more robust than that of pure EP, with an ID/IG value of 2.03, indicating the highest degree of graphitization.

Keywords: *9,10-Dihydro-9-oxa-10-phosphaphenanthrene-10-oxide; 2-Aminobenzothiazole; Indole-3-carboxaldehyde; Multielement synergistic flame retardant*

Received on 02 March 2023, Accepted on 28 May 2023, Published on 15 July 2023

1 Introduction

Epoxy resin (EP) is a thermosetting material widely utilized in polymer composites, coatings, construction, automotive, and aerospace industries due to its excellent adhesion, good chemical resistance, outstanding mechanical properties, and processability. Bisphenol A diglycidyl ether (DGEBA)-type EP is the most prevalent variant. However, akin to most organic polymers, DGEBA-type EP lacks inherent flame retardancy[3]. Its aromatic structures and carbon-hydrogen chains lead to the release of substantial heat and toxic gases upon combustion[4], posing severe threats to human life and property safety. The flammability of EP restricts its development across various fields; thus, enhancing its flame-retardant performance is of great significance.

Methods to improve the flame retardancy of EP are primarily categorized into reactive and additive types[6-7]. The reactive approach involves covalently bonding flame-retardant elements into the EP macromolecular chain via monomers or curing agents[8]. The additive approach directly blends flame retardants into the EP matrix without chemical reactions. This method is simple, cost-effective, and better suited for large-scale industrial production and commercial applications compared to reactive flame retardants.

Traditional halogen-based flame retardants have been employed to impart flame retardancy to EP[9]. Although effective, they generate environmentally and biologically hazardous toxic gases during combustion[10] and are gradually being replaced by halogen-free alternatives. In recent years, driven by increasing environmental demands, a series of halogen-free flame retardants has emerged[11-12]. Among these, phosphorus-containing flame retardants exhibit broad application prospects due to their low toxicity and high designability[13]. Phosphorus-based flame retardants are environmentally friendly, offering excellent flame-retardant performance[14] while producing fewer toxic gases and smoke during combustion. To date, derivatives of 9,10-dihydro-9-oxa-10-phosphaphenanthrene-10-oxide (DOPO)[15] and ammonium polyphosphate (APP) have been widely applied in EP flame retardancy.

Phosphorus-based flame retardants function in both the condensed and gas phases during polymer combustion. In the condensed phase, the decomposing flame retardant produces phosphoric acid or polyphosphoric acid, which catalyzes char formation[17]. This char layer covers the substrate surface, effectively insulating oxygen[18] and hindering heat transfer between the polymer and the flame[19]. In the gas phase, the flame retardant releases phosphorus-containing radicals during combustion, which capture H· and OH· radicals, quenching the combustion chain reaction[20] and thereby delaying or interrupting burning. However, to achieve satisfactory flame-retardant effects, high loadings of most phosphorus-based flame retardants are often required, which can deteriorate the mechanical properties of EP composites. Recently, multi-element flame-retardant systems—introducing other elements such as N, B, and S—have been designed to effectively synergize and enhance EP flame retardancy.

DOPO is a common, low-cost phosphorus-based flame retardant that has become a crucial intermediate for organophosphorus flame retardants[21]. It has garnered significant attention due to its versatile structure achievable through functionalization and excellent flame-retardant activity[22]. The active P–H bond in the DOPO structure readily reacts with various electron-deficient compounds to form diverse DOPO derivatives[23]. Therefore, based on DOPO, different flame-retardant elements and groups—such as P/N/B[24], P/N/Si[25], and P/N/S[26] moieties—can be conveniently integrated into a single compound. These derivatives can be added as additives to the epoxy matrix to impart flame retardancy. Zhang et al.[27-28] designed a DOPO derivative (DST) constructed from sulfaguanidine and thiophene, employing it as a co-curing agent for EP. In vertical burning tests, EP containing less than 5 wt% DST achieved a UL-94 V-0 rating with an LOI value of 32.8%. Compared to pure EP, its peak heat release rate (PHRR) and total heat release (THR) decreased by 31.2% and 18.8%, respectively. Indole-3-carboxaldehyde (I3C) contains an aldehyde group capable of reacting with the primary amine group of 2-aminobenzothiazole (ABZ) to form a Schiff base, which subsequently reacts readily with the P–H group of DOPO to yield a flame-retardant derivative containing P, N, and S.

Inspired by the chemical structure of DOPO and the concept of multi-element synergistic flame retardancy, a structurally analogous DOPO-based (DAI) flame retardant was designed and applied to EP in this study. The DAI flame retardant, derived from DOPO, I3C, and ABZ, was synthesized via a two-step reaction. EP was then modified by blending with DAI. The chemical structure of DAI was characterized. The thermal decomposition behavior of the epoxy thermoset was studied, and flammability and combustion experiments were conducted to evaluate the flame-retardant performance, combustion behavior, and mechanism of the flame-retardant epoxy thermoset.

2 Experimental Section

2.1 Instruments and Reagents

iCone Classic cone calorimeter (Fire Testing Technology Ltd., UK); JNM-ECZ600R/S1 nuclear magnetic resonance spectrometer (NMR, JEOL Ltd., Japan); DXR2xi micro-Raman imaging spectrometer (Raman, Thermo Fisher Scientific Inc., USA); HITACHI Regulus8100 cold field emission scanning electron microscope (FESEM, Hitachi Ltd., Japan); NICOLET IS10 Fourier transform infrared spectrometer (FT-IR, Thermo Fisher Scientific Inc., USA); SDT Q50 thermogravimetric analyzer (TGA, TA Instruments, USA); DZF-6020 vacuum drying oven (Shanghai Boxun Industrial Co., Ltd.); DF-101S constant temperature magnetic stirring oil bath (Zhengzhou Great Wall Industrial and Trade Co., Ltd.); KQ5200DE numerical control ultrasonic cleaner (Kunshan Ultrasonic Instrument Co., Ltd.);

HS-JF-3 limiting oxygen index meter (Shanghai Hesheng Instrument Technology Co., Ltd.); HS-RSJ vertical burning tester (Shanghai Hesheng Instrument Technology Co., Ltd.).

DOPO, ABZ, I3C, ethanol (99.7%), and 4,4'-diaminodiphenylmethane (DDM) were analytical grade reagents purchased from Shanghai Macklin Biochemical Co., Ltd. EP (E-51, epoxy value 0.51) was procured from Nan Ya Epoxy Resin (Kunshan) Co., Ltd.

2.2 Preparation of DAI Flame Retardant Intermediate A-I

ABZ (15 g) was placed in a two-necked flask, followed by the addition of ethanol (100 mL) as the solvent. The mixture was magnetically stirred to ensure complete dispersion of ABZ in the ethanol solvent. Under continuous stirring, pre-weighed I3C (14.5 g, molar ratio n(ABZ):n(I3C) = 1:1) was slowly added. The mixture was then heated to 85 °C and stirred continuously for 10 h, followed by natural cooling to room temperature. Finally, the product was isolated via filtration using a Büchner funnel, dried in an oven at 60 °C for 24 h, yielding 25.6 g of a yellow powder (A-I) with a yield of 92.4%. The molecular formula of A-I is $C_{16}H_{11}N_3S$. The product was stored for subsequent use.

2.3 Preparation of DAI

DOPO (21.6 g) was placed in a two-necked flask, and ethanol (100 mL) was added as the solvent. The DOPO-ethanol mixture was subjected to ultrasonication to accelerate DOPO dissolution. After dissolution, the flask containing the clear solution was immersed in an oil bath preheated to 85 °C and magnetically stirred. Pre-weighed intermediate A-I was slowly added under stirring. After continuous stirring for 12 h, the mixture underwent rotary evaporation. The resulting product was filtered, washed, and separated to remove unreacted DOPO and A-I. Finally, the product was dried in an oven at 60 °C for 24 h, yielding 45.1 g of a light-yellow powder (DAI) with a yield of 91.5%.

2.4 Preparation of EP/DAI Blended Samples

EP (21.6 g) was placed in a polytetrafluoroethylene beaker, followed by the addition of the curing agent DDM (10 g). The mixture was then heated and stirred in an oil bath to enhance EP fluidity, facilitating the addition and blending of the flame retardant. Subsequently, DAI (27.9 g) was slowly added. After thorough mixing, the blend was poured into molds of specific dimensions required for cone calorimetry, LOI, vertical burning, and tensile mechanical testing. The samples were cured in an oven following a temperature gradient: 100 °C for 2 h, 120 °C for 2 h, and 150 °C for 2 h, yielding the EP/DAI blended samples. The formulation of materials used in the experiment is listed in Table 1. The reaction scheme and preparation process of DAI are illustrated in Fig. 1A.

Table 1 Formula of EP/DAI flame retardant composite

Sample	w(EP)/%	w(DDM)/%	w(DAI)/%	w(P)/%	w(N)/%
EP	80.00	20.00	0.00	0.00	0.00
EP/DAI-3	77.60	19.40	3.00	0.19	0.26
EP/DAI-5	76.00	19.00	5.00	0.31	0.43
EP/DAI-7	74.40	18.60	7.00	0.44	0.60

2.5 Sample Characterization

2.5.1 FT-IR Spectroscopy

Fourier transform infrared spectroscopy was employed to analyze the structural composition and functional groups of different substances. The scanning range was 4000–400 cm^{-1}, with a resolution of 4 cm^{-1} and 32 scans. Prior to characterization, samples were mixed with potassium bromide (KBr) powder and pressed into pellets.

2.5.2 NMR Spectroscopy

Nuclear magnetic resonance spectroscopy was utilized to analyze the chemical structure of the samples. Approximately 5–10 mg of the sample was weighed into a test tube and dissolved in CCl_4. The solution was transferred into an NMR tube and subjected to ^{1}H NMR analysis to obtain the ^{1}H NMR spectrum.

2.5.3 TGA Analysis

The thermal stability of the EP composites was evaluated using a thermogravimetric analyzer under a nitrogen atmosphere. The temperature range was 30–800 °C, with a heating rate of 10 °C/min. The mass of each sample was 5–10 mg.

2.5.4 Cone Calorimeter Test (CCT)

According to ISO 5660 standards, a cone calorimeter was used to assess the combustion behavior of the EP composites. The incident heat flux was set at 35 kW/m². Sample dimensions were 100 mm × 100 mm × 4 mm. Reported data represent the average of three measurements.

2.5.5 LOI Test

The LOI values of the EP composites were measured using a limiting oxygen index meter according to ASTM D2863-06. Sample dimensions were 130 mm × 6.5 mm × 3.2 mm.

2.5.6 Vertical Burning Test

UL-94 vertical burning tests were conducted using a vertical burning tester according to GB/T 2408-2008 to evaluate the flammability of the EP composites. The combustion process was documented via photography at specified intervals. Sample dimensions were 130 mm × 13 mm × 3.2 mm.

2.5.7 SEM Analysis

Scanning electron microscopy was employed to observe the micromorphology of the residues after combustion. Samples were examined at an acceleration voltage of 5 kV. Prior to testing, samples were sputter-coated with gold to improve conductivity.

2.5.8 Micro-Raman Imaging Spectroscopy

Raman spectroscopic analysis of the char residues from the EP composites was performed at room temperature. Within the range of 600–2400 cm^{-1}, the degree of graphitization was analyzed based on the ratio of the intensities of the D-band (ID) and G-band (IG).

3 Results and Discussion

3.1 Structural Analysis of DAI

The synthetic route of the N/P-containing DAI flame retardant is depicted in Fig. 1A. To obtain a higher purity DAI product, the synthesis was conducted in two steps. The synthesized DAI flame retardant was characterized by FT-IR and NMR to confirm its structure. The FT-IR spectra of DOPO, I3C, ABZ, and DAI are presented in Fig. 1B. The characteristic peak observed at 1810 cm^{-1} corresponds to the –CHO group in I3C but is absent in DAI, indicating the participation of the –CHO group in the reaction. The characteristic peak of the P–H bond in DOPO appears at 2437 cm^{-1} but vanishes in DAI, suggesting that the P–H bond reacted with the C=N bond. Furthermore, the N–H bond (3000–3400 cm^{-1}) and the P–O bond (1237 cm^{-1}) of DOPO are retained in DAI, corroborating the successful reaction of DOPO with I3C and ABZ. The ^{1}H NMR spectrum of DAI is shown in Fig. 1C. The resonance signal of the N–H bond appears near δ 9.2, while the doublet signal corresponding to hydrogen atoms attached to the C–H bond appears near δ 5.85. Additionally, signals in the δ 6.5–8.0 range and multiplet signals near δ 8.3

arise from aromatic protons. Moreover, the integral values of these signals are 1.88, 1.00, and 16.89, respectively. Simplifying these to the smallest integer ratio yields the proportion of H atoms in the N–H, C–H, and aromatic environments, consistent with the theoretical ratios for the synthesized DAI. In summary, the aforementioned results confirm the chemical structure of the DAI flame retardant and its successful synthesis.

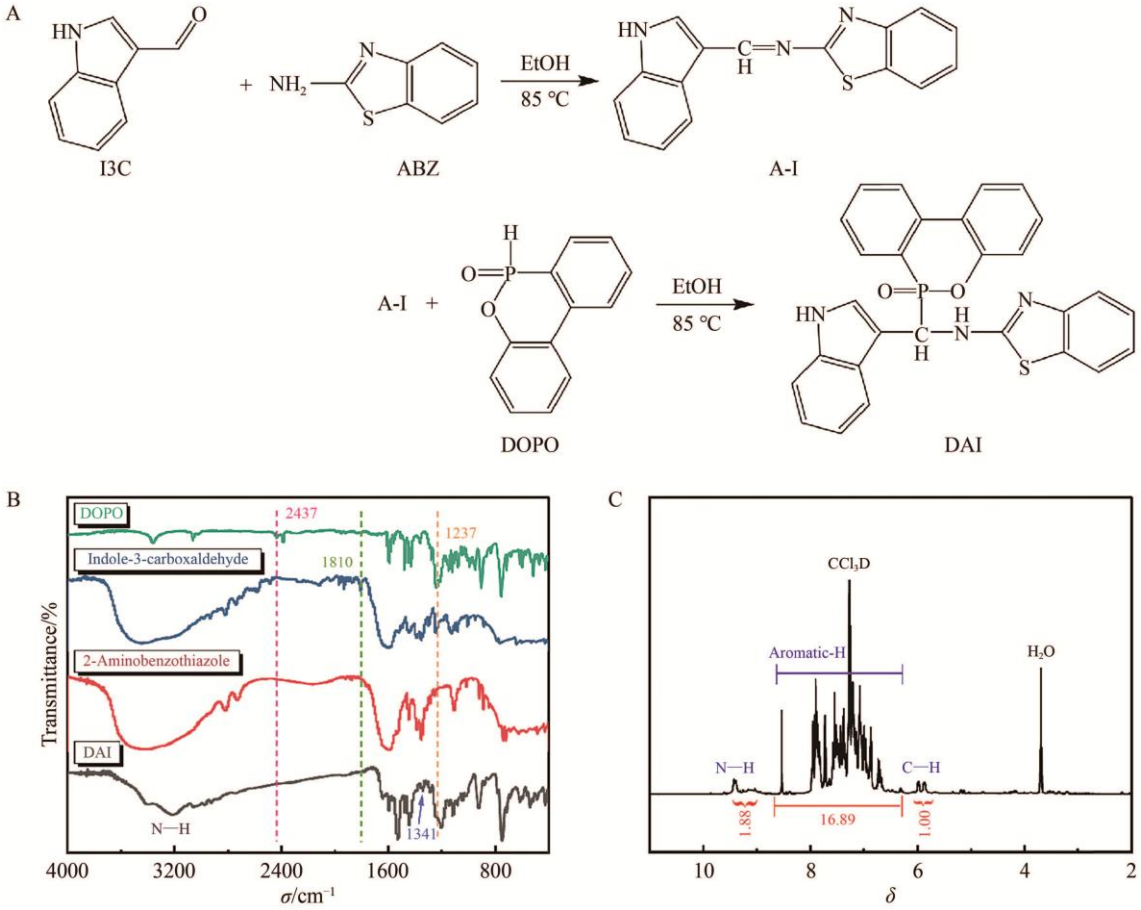

Figure 1 (A) Schematic diagram of synthesized DAI; (B) FT-IR spectra of DAI and DOPO, I3C, and ABZ; (C) ^{1}H NMR spectrum of DAI

3.2 Thermal Stability Analysis of EP Composites

The effect of DAI loading on the thermal stability of EP was investigated using TGA under a N_2 atmosphere. The TG and DTG curves of EP, EP/DAI-3, EP/DAI-5, and EP/DAI-7 are presented in Fig. 2. Relevant thermal degradation data, including the temperatures at 5% mass loss (T_5%) and 10% mass loss (T_{10}%), maximum mass loss rate, and char residue at 800 °C, are listed in Table 2. As shown in Fig. 2, both EP and its composites exhibit single-step decomposition characteristics. Compared to pure EP (T_5% = 370.8 °C), the initial decomposition temperatures of EP/DAI-3 (T_5% = 354.8 °C), EP/DAI-5 (T_5% = 350.2 °C), and EP/DAI-7 (T_5% = 352.7 °C) are lower, attributed to the catalytic nature of DAI. Concurrently, the T_{10}% of the EP composites decreases with increasing DAI content. Notably, the incorporation of DAI reduces the maximum mass loss rate of the EP composites. Among the different loadings, the composite with 3 wt% DAI exhibits the highest maximum mass loss rate, while that with 5 wt% shows the lowest. This might be because an excessive amount of DAI in the 7 wt% composite hinders uniform dispersion within the epoxy resin, adversely affecting char layer quality and structure. Excess DAI may also disrupt the molecular structure and cross-linking network of EP, leading to decreased thermal stability. Furthermore, at 800 °C, the char residues of EP/DAI-3, EP/DAI-5, and EP/DAI-7 are higher than that of pure EP due to the presence of DAI promoting char formation. Phosphorus-based acidic species generated from DAI degradation likely facilitate the formation of a phosphorus-rich char layer, thermally insulating the underlying matrix and inhibiting thermal degradation. The relatively minor differences in the initial decomposition

temperatures among the three EP composites with varying DAI contents suggest that the added amounts did not significantly compromise the inherent thermal stability of EP.

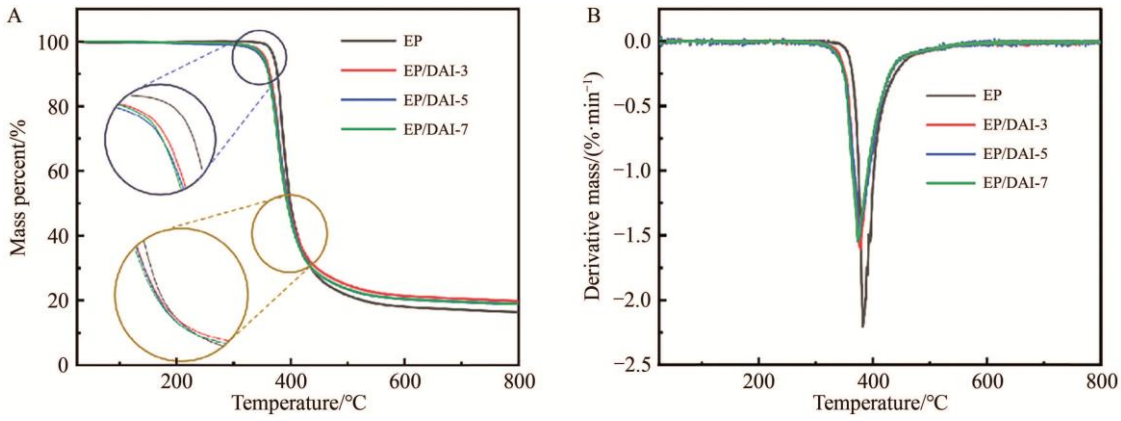

Figure 2 Fig. 2 (A) TG and (B) DTG curves at N_2 atmospheres of EP, EP/DAI-3, EP/DAI-5, and EP/DAI-7

Table 2 Data of TGA test

Sample	Char residue at 800 ℃/%	T_5%/℃	T_{10}%/℃	Maximum mass loss rate/(%·℃$^{-1}$)
EP	16.4	370.8	376.5	2.20
EP/DAI-3	19.8	354.8	363.8	1.61
EP/DAI-5	18.9	350.2	361.3	1.50
EP/DAI-7	19.0	352.7	361.2	1.54

3.3 Flame-Retardant Performance Analysis of EP Composites

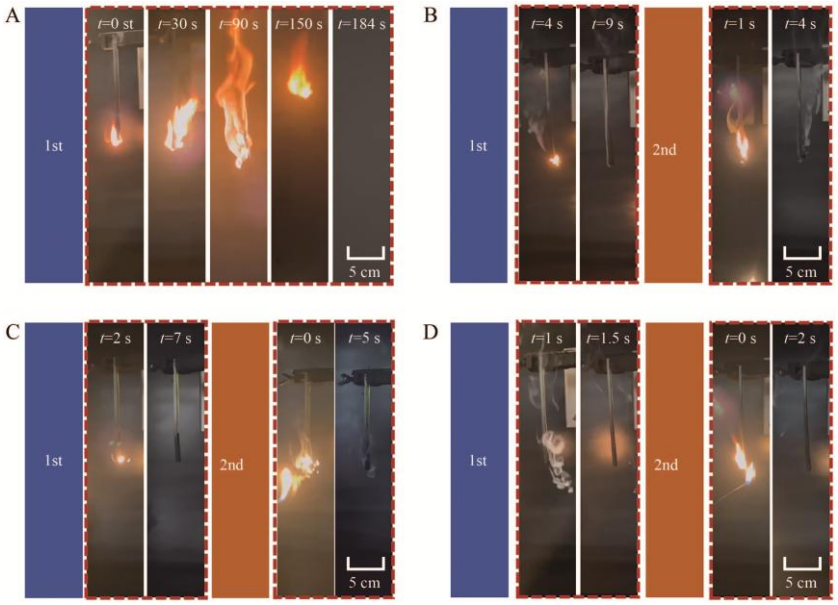

Figure 3 UL-94 test of (A) EP, (B) EP/DAI-3, (C) EP/DAI-5, and (D) EP/DAI-7

As shown in Fig. 3A, during the UL-94 test, pure EP burned violently after the first ignition, accompanied by severe flaming droplets and substantial smoke release, failing to self-extinguish, consistent with its highly flammable nature[29]. Consequently, pure EP received no rating. Upon adding 3, 5, and 7 wt% DAI to EP, EP/DAI-3 (Fig. 3B), EP/DAI-5 (Fig. 3C), and EP/DAI-7 (Fig. 3D) all eliminated flaming drips and self-extinguished shortly after the first ignition. EP/DAI-3 and EP/DAI-5 exhibited rapid self-extinguishing capabilities of 4 s and 5 s, respectively, after the second ignition, earning them a UL-94 V-1 rating. EP/DAI-7 demonstrated superior self-extinguishing ability, extinguishing 1.5 s after the first ignition and 2 s after the second ignition, achieving a UL-94 V-0 rating. Furthermore, as depicted in Fig. 4, the addition of DAI significantly enhanced the LOI values of the EP composites. EP/DAI-7 exhibited the highest LOI value of 32.6%, surpassing EP/DAI-5 (30.1%), EP/DAI-3 (28.8%), and pure EP (24.4%). This indicates the remarkable flame-retardant efficiency of DAI, conferring outstanding flame-retardant properties to the EP composites.

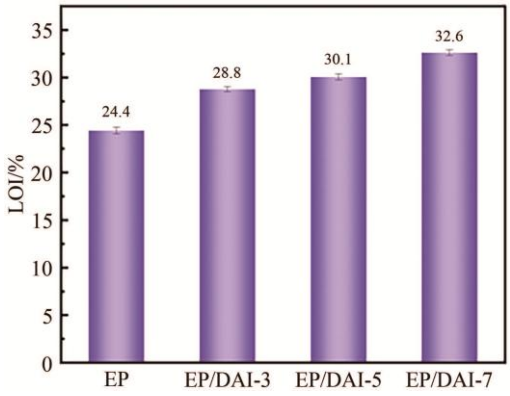

Figure 4 LOI values of EP, EP/DAI-3, EP/DAI-5, and EP/DAI-7

The cone calorimeter test (CCT) is an effective method for evaluating the combustion parameters of materials under realistic fire conditions. The CCT results for EP and its composites are presented in Fig. 5, with detailed data listed in Table 3, including time to ignition (TTI), peak heat release rate (pHRR), total heat release (THR), peak smoke production rate (pSPR), total smoke production (TSP), peak CO production rate (pCOPR), and peak CO_2 production rate (pCO_2PR). The TTI of pure EP was 115 s. In contrast, the TTIs of EP composites containing DAI were shorter than that of pure EP and exhibited a decreasing trend with increasing DAI content, indicating that the DAI flame retardant promotes the degradation and charring of the EP composites. From Fig. 5A, 5B, and Table 3, the pHRR and THR of pure EP reached 1004.7 kW/m² and 81.1 MJ/m², respectively. Upon introduction of the DAI flame retardant, both pHRR and THR of the EP composites decreased to varying extents. Notably, for EP/DAI-7, the pHRR and THR decreased to 657.2 kW/m² and 67.7 MJ/m², representing reductions of 34.5% and 16.5%, respectively. This demonstrates that incorporating DAI significantly suppresses heat release during combustion, with the DAI loading being a key factor influencing the HRR of EP composites.

Table 3 CCT data of EP, EP/DAI-3, EP/DAI-5, and EP/DAI-7 composites

Samples	TTI/s	pHRR/(kW·m^{-2})	THR/(MJ·m^{-2})	pSPR/(m^2·s^{-1})	TSP/m^2	pCOPR/(g·s^{-1})	pCO_2PR/(g·s^{-1})
EP	115	1004.7	81.1	0.28	26.5	0.034	0.64
EP/DAI-3	90	992.8	61.7	0.26	21.8	0.040	0.63
EP/DAI-5	96	763.7	65.7	0.34	26.8	0.039	0.45
EP/DAI-7	80	657.2	67.7	0.23	29.1	0.023	0.37

Moreover, in real fires, smoke and toxic gases are often the most lethal factors[31], accounting for the majority of fire-related casualties[32]. Smoke parameters such as pSPR and TSP of EP and its composites were used to evaluate smoke release behavior. From Fig. 5C, 5D, and Table 3, the pSPR and TSP values of pure EP were 0.28

m²/s and 26.5 m², respectively. EP/DAI-7 with 7% DAI showed a reduced pSPR of 0.23 m²/s, the lowest among all composites, representing a 17.8% decrease compared to pure EP. Notably, compared to pure EP, the TSP of EP/DAI-3 was effectively suppressed, whereas those of EP/DAI-5 and EP/DAI-7 increased. This suggests that increasing DAI content inhibits the smoke production rate but elevates the total smoke release of the EP composites. From Fig. 5E, 5F, and Table 3, compared to pure EP, EP/DAI-3, and EP/DAI-5, EP/DAI-7 exhibited significant reductions in pCOPR and pCO_2PR during combustion. The pCOPR decreased from 0.034 g/s (pure EP) to 0.023 g/s, and the pCO_2PR decreased from 0.64 g/s to 0.37 g/s, reductions of 32.3% and 42.2%, respectively. This indicates that EP/DAI-7 effectively suppresses the release of CO and CO_2, likely due to the formation of a denser char layer that more efficiently impedes their release.

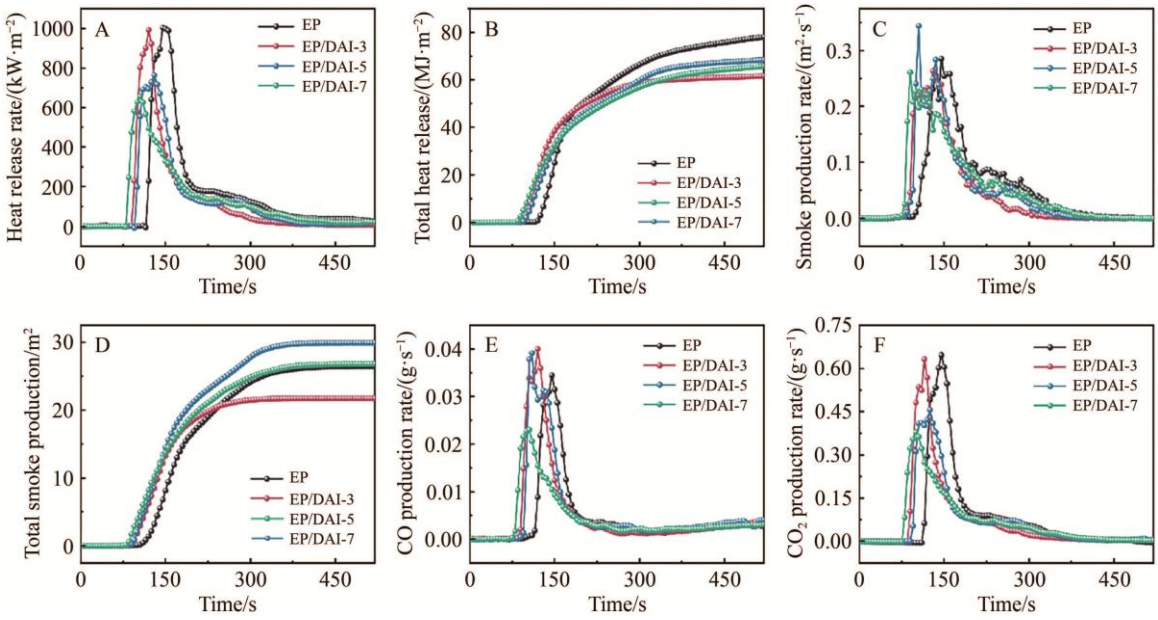

Figure 5 （A） HRR，（B） THR，（C） SPR，（D） TSP，（E） COPR，（F） CO2PR curves of EP， EP/DAI-3， EP/DAI-5 and EP/DAI-7

The aforementioned CCT results demonstrate that DAI significantly enhances the flame-retardant performance of EP composites. The DAI loading exerts a substantial influence on suppressing smoke and toxic gas release, with 7 wt% DAI exhibiting superior fire safety. This indicates that modifying epoxy resin with DAI is an effective pathway to improve the flame-retardant properties of EP composites.

3.4 Char Residue Analysis of EP Composites

To elucidate the flame-retardant mechanism of DAI-modified EP, the morphology and structure of the char residues formed during combustion were investigated for pure EP, EP/DAI-3, EP/DAI-5, and EP/DAI-7. Fig. 6A presents digital photographs of the residues after CCT. The residue from pure EP appeared loose and friable. Upon adding DAI, the char residues became compact, continuous, and cohesive, without exposing the underlying aluminum foil, indicating that a high-quality char layer forms as a protective barrier during practical combustion. To further understand the mechanism, the surface morphology of the char residues post-CCT was analyzed via SEM (Fig. 6B). The char residues of EP and EP/DAI-3 were loose and fragile, lacking a continuous char layer, rendering the internal structure unstable and easily crumbling into powder upon slight contact. The char residue of EP/DAI-5 began to show continuity and block-like structures, yet numerous cracks were visible on its surface, indicating insufficient robustness. In contrast, the char layer of EP/DAI-7 exhibited a dense and compact microstructure, suggesting that increasing DAI loading facilitates the formation of a sturdier char layer during EP combustion. This dense char layer acts as an effective thermal insulator, protecting the underlying EP from heat and oxygen, thereby achieving enhanced flame retardancy.

Furthermore, the degree of graphitization of the char residues was assessed via Raman spectroscopy (Fig. 6C). Two distinct peaks are observable at approximately 1346 cm^{-1} (D band) and 1581 cm^{-1} (G band), confirming the

presence of a graphitic structure in the char[34]. Generally, the degree of graphitization is determined by comparing the areas of the D and G bands in the Raman spectrum[35]. The ID/IG ratio reflects the graphitization level; a lower value corresponds to a higher degree of graphitization. Enhanced graphitization improves the protection of the internal matrix against combustion, contributing to effective flame retardancy[36]. In this study, the ID/IG values for EP, EP/DAI-3, EP/DAI-5, and EP/DAI-7 were 2.62, 2.39, 2.31, and 2.03, respectively. EP/DAI-7 exhibited the lowest ID/IG value, indicating the highest degree of graphitization among the residues. In other words, EP/DAI-7 formed the most stable char layer on its surface during combustion, inhibiting further mass and gas transfer, thereby conferring excellent smoke suppression and flame-retardant properties. With increasing DAI loading, the ID/IG values of the char layers gradually decreased, demonstrating that DAI incorporation improves char layer quality, favoring the formation of a more robust char layer during EP combustion.

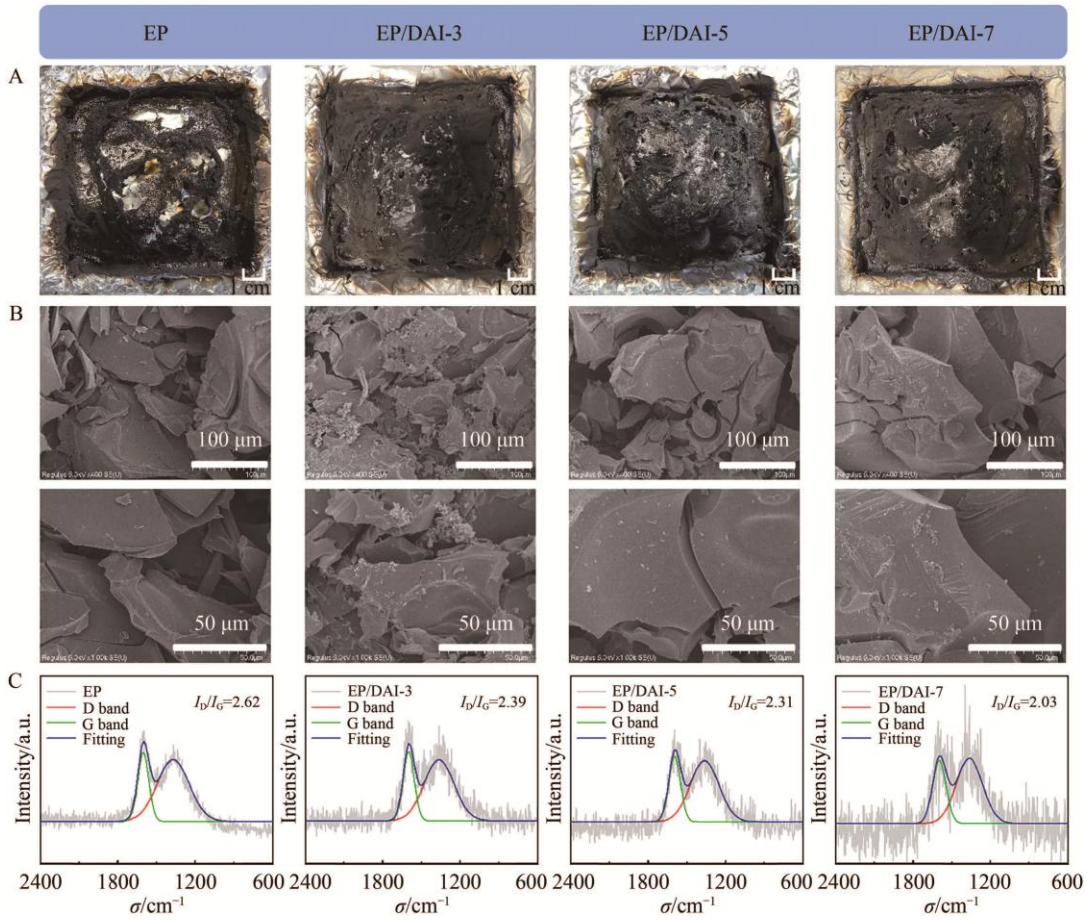

Figure 6 A) Digital photographs, (B) SEM photographs, and (C) Raman spectra of the char residues of EP, EP/DAI-3, EP/DAI-5, and EP/DAI-7

The exceptional flame-retardant and smoke-suppression performance of the DAI-modified epoxy resin (EP) composites stems from the synergistic integration of multi-element chemistry, condensed-phase char formation, and gas-phase radical quenching, effectively resolving the trade-off between low additive loading and high fire safety in traditional phosphorus-based systems. Structurally, the DAI molecule—synthesized via a two-step Schiff base reaction between DOPO, 2-aminobenzothiazole (ABZ), and indole-3-carboxaldehyde (I3C)—incorporates P, N, and S heteroatoms into a single molecular framework, as confirmed by FT-IR (disappearance of P–H and –CHO peaks) and ^{1}H NMR (consistent aromatic proton integration ratios). This molecular design enables dual-mode flame retardancy: in the condensed phase, thermal decomposition of DAI at relatively low temperatures (T_5% = 350 – 355 °C) generates phosphoric and polyphosphoric acid species, which catalyze dehydration and cross-linking of the EP matrix to form a dense, phosphorus-rich char layer. The presence of N- and S-containing moieties further enhances char stability: N elements release inert gases (e.g., NH_3, N_2) that swell the char into a foam-like structure, while S enhances cross-linking density via sulfur-oxygen interactions,

preventing char cracking. SEM analysis of post-combustion residues confirms this evolution: pure EP yields a loose, friable char, whereas EP/DAI-7 forms a continuous, crack-free layer that fully covers the underlying substrate. Raman spectroscopy further reveals that the DAI-derived char exhibits the lowest I_D/I_G ratio (2.03 vs. 2.62 for pure EP), indicating the highest degree of graphitization—a critical factor in improving thermal insulation and mechanical robustness of the protective barrier. In the gas phase, the P–H bond cleavage during DAI decomposition releases phosphorus-containing radicals (PO•, PO_2•) that quench high-energy H• and OH• radicals, interrupting the combustion chain reaction. This dual-phase synergy is quantitatively validated by cone calorimetry: EP/DAI-7 achieves a 34.5% reduction in peak heat release rate (pHRR, 657.2 vs. 1004.7 kW/m² for pure EP), alongside 32.3% and 42.2% decreases in peak CO and CO_2 production rates (pCOPR and pCO_2PR), respectively. Notably, the 7 wt% DAI loading optimizes char quality: lower loadings (3–5 wt%) result in incomplete char coverage, while excessive DAI (beyond 7 wt%) causes agglomeration, disrupting EP cross-linking and reducing char integrity. The multi-element synergy also mitigates the "phosphorus migration" issue common in single-element systems, as the covalent integration of P, N, and S into DAI prevents leaching and ensures sustained flame-retardant activity. This combination of molecular design, condensed-phase char enhancement, and gas-phase radical scavenging enables EP/DAI-7 to achieve an LOI of 32.6% and a UL-94 V-0 rating, outperforming most reported DOPO-based additives at comparable loadings.

While the DAI flame retardant demonstrates remarkable efficacy in EP composites, several critical avenues warrant further exploration to advance its practical deployment and expand its utility in sustainable polymer applications. First, the current study focuses on bulk EP composites; future work should investigate DAI's performance in fiber-reinforced EP laminates (e.g., carbon fiber/epoxy, glass fiber/epoxy), which are widely used in aerospace and automotive sectors, to assess how fiber-matrix interfaces affect char formation and flame retardancy. Second, the long-term durability of DAI-modified EP remains uncharacterized: accelerated aging tests (thermal, UV, and humidity exposure) are needed to evaluate whether DAI leaches or degrades over time, potentially compromising fire safety. Third, the current synthesis uses ethanol as a solvent; replacing it with greener alternatives (e.g., water or bio-based alcohols) and optimizing reaction conditions (e.g., microwave-assisted synthesis) could reduce environmental footprint and production costs, aligning with circular economy principles. Fourth, expanding the multi-element synergy concept to incorporate additional elements (e.g., Si, B) could further enhance char stability and reduce total smoke production (TSP), which increases slightly in EP/DAI-7 (29.1 vs. 26.5 m² for pure EP) despite lower smoke production rates. For instance, integrating Si–O bonds could form ceramic-like char layers with superior thermal insulation, while B-containing moieties might catalyze earlier char formation. Fifth, mechanistic studies would benefit from in situ characterization techniques: in situ FT-IR and TGA-MS could track real-time gas evolution and char precursor formation, while synchrotron-based X-ray tomography could map 3D char microstructure to correlate porosity with flame-retardant efficiency. Sixth, computational modeling (e.g., density functional theory, molecular dynamics simulations) could elucidate the electronic interactions between P, N, and S atoms in DAI, predicting optimal heteroatom ratios and molecular architectures for enhanced synergy. Seventh, practical applications require compatibility with industrial processing: investigating DAI's impact on EP curing kinetics (e.g., gel time, cure temperature) and mechanical properties (flexural strength, impact resistance) is essential to ensure the composites meet industrial performance standards. Eighth, regulatory compliance and environmental safety must be addressed: toxicity assays (e.g., zebrafish embryo toxicity, biodegradability tests) are needed to confirm DAI's eco-friendliness, particularly given the presence of S-containing benzothiazole moieties. Finally, scaling up DAI production from laboratory to pilot scale presents challenges in maintaining product purity and consistency; continuous flow synthesis methods could improve reproducibility and reduce batch-to-batch variability. By addressing these fundamental and applied research gaps, DAI could evolve from a laboratory-scale additive to a commercially viable flame retardant, contributing to the development of safer, more sustainable polymer materials for high-performance applications.

4 Conclusion

A novel multielement synergistic flame retardant, DAI, was successfully synthesized via a two-step reaction using DOPO, ABZ, and I3C. Its successful synthesis was confirmed by FT-IR and NMR spectroscopy. DAI was blended with epoxy resin via a thermosetting method to enhance the fire safety of the EP composites. The results indicate that EP composites incorporating DAI effectively suppress the release of heat, smoke, and toxic gases during

combustion. Compared to pure EP, EP/DAI-7 exhibited outstanding smoke suppression and flame-retardant performance, demonstrating superior fire safety. CCT results revealed that EP/DAI-7, with 7 wt% DAI loading, achieved the lowest pHRR (657.2 kW/m²), pCOPR (0.023 g/s), and pCO_2PR (0.37 g/s) compared to loadings of 3% and 5%. Concurrently, EP/DAI-7 attained an LOI value of 32.6% and a UL-94 V-0 rating. Finally, the flame-retardant mechanism of EP/DAI was analyzed. SEM and Raman analyses indicated that the char residue of EP/DAI-7 was denser and more robust than those of pure EP, EP/DAI-3, and EP/DAI-5, with the lowest ID/IG value of 2.03, signifying the highest degree of graphitization. In summary, incorporating DAI into EP composites represents an effective strategy to enhance their flame-retardant performance and fire safety.

References

[1] WANG G F, LI H F, SHAO Y R, et al. Preparation method of biogenic phytic acid and chitosan-related epoxy resin flame retardant: a review[J]. J Polym Res, 2021, 30(7): 269.

[2] MATHEWS L D, CAPRICHO J C, PEERZADA M, et al. Recent progress and multifunctional applications of fire-retardant epoxy resins[J]. Mater Today Commun, 2022, 33: 104702.

[3] XIAO Z T, WU G L, YANG T M, et al. Sustainably sourced and DOPO-derived triols as hardeners for epoxy thermosets: a promising solution to synchronously improve flame retardancy, mechanical strength and toughness[J]. Chem Eng J, 2022, 498: 155484.

[4] ZHANG Y B, YAN H X, FENG G P, et al. Non-aromatic Si, P, N-containing hyperbranched flame retardant on reducing fire hazards of epoxy resin with desirable mechanical properties and lower curing temperature [J]. Compos Part B, 2021, 222: 109043.

[5] ZHOU C Y, WU K X, ZHANG Y, et al. Alginic acid derivatives/DOPO modified epoxy resins: excellent flame retardancy, mechanical properties, chemical resistance[J]. Polym Degrad Stab, 2022, 225: 110778.

[6] YU Y Y, TANG S, FENG D, et al. Non-covalently functionalized black phosphorene to efficient flame retardant EVA with improved mechanical properties[J]. Polym Degrad Stab, 2022, 225: 110777.

[7] PHAM L H, NGUYEN N T, NGUYEN D M, et al. Effective non-halogen flame-retardants combined with $nSiO_2$ particles to improve thermal stability and fire resistance of high-performance polyurethane nanocomposite foams[J]. J Mater Sci Technol, 2022, 203: 1-13.

[8] RAD E R, VAHABI H, DE ANDA A R, et al. Bio-epoxy resins with inherent flame retardancy[J]. Prog Org Coat, 2019, 135: 608-612.

[9] WANG P, CHEN L, XIAO H, et al. Nitrogen/sulfur-containing DOPO based oligomer for highly efficient flame-retardant epoxy resin[J]. Polym Degrad Stab, 2020, 171: 109023.

[10] LIN Y, CHEN J L, LI H Z. Flame retardant properties of tannic acid/poly(vinyl alcohol)[J]. Chin J Appl Chem, 2021, 40(1): 69-78.

[11] KANDOLA B K, MAGNONI F, EBDON J R. Flame retardants for epoxy resins: application-related challenges and solutions[J]. J Vinyl Addit Technol, 2022, 28(1): 17-49.

[12] CHEN Q, WANG S, LI S X, et al. Highly efficient phosphorous-containing flame retardant for transparent epoxy resin with good mechanical properties[J]. J Polym Res, 2021, 30(1): 32.

[13] YANG Y X, WANG D Y, JIAN R K, et al. Chemical structure construction of DOPO-containing compounds for flame retardancy of epoxy resin: a review[J]. Prog Org Coat, 2021, 175: 107316.

[14] SHI J J, SHI Z H, LI H Z. Preparation of magnesium aluminum-type hydrotalcite compounds intercalated with phosphorus flame retardants and their flame retardant application in thermoplastic polyurethane[J]. Chin J Appl Chem, 2021, 40(9): 1288-1301.

[15] WANG P, CHEN L, XIAO H. Flame retardant effect and mechanism of a novel DOPO based tetrazole derivative on epoxy resin[J]. J Anal Appl Pyrolysis, 2019, 139: 104-113.

[16] ZOU Y B, SHI J J, CUI W Q, et al. Isopropanolamine-modified ammonium polyphosphate for improved flame retardancy of epoxy resin[J]. J Appl Polym Sci, 2022, 141(25): e55526.

[17] KIM H H, SIM M J, LEE J C, et al. The effects of chemical structure for phosphorus-nitrogen flame retardants on flame retardant mechanisms[J]. J Mater Sci, 2021, 58: 6850-6864.

[18] YUAN Y, SHI Y Q, YU B, et al. Facile synthesis of aluminum branched oligo(phenylphosphonate) submicro-particles with enhanced flame retardance and smoke toxicity suppression for epoxy resin composites[J]. J Hazard Mater, 2020, 381: 121233.

[19] SHEN J J, LIANG J W, LIN X F, et al. The flame-retardant mechanisms and preparation of polymer composites and their potential application in construction engineering[J]. Polymers, 2022, 14(1): 82.

[20] QIN C L, CHEN J, RUAN S S, et al. Theoretical study on the effect of oxidation states of phosphorus flame r etardants on their mode of action[J]. Polym Degrad Stab, 2022, 223: 110735.
[21] PENG W, NIE S B, XU Y X, et al. A tetra-DOPO derivative as highly efficient flame retardant for epoxy resins [J]. Polym Degrad Stab, 2021, 193: 109715.
[22] GUO W W, YU B, YUAN Y, et al. In situ preparation of reduced graphene oxide/DOPO-based phosphonami date hybrids towards high-performance epoxy nanocomposites[J]. Compos Part B, 2017, 123: 154-164.
[23] SHI Z H, LUO F B, LI H Z, et al. Synthesis of a graft-functionalized flame retardant based on DOPO and its a pplication on the surface of terylene/cotton fabrics[J]. J Appl Polym Sci, 2022, 141(8): 54976.
[24] HUO S Q, SAI T, RAN S Y, et al. A hyperbranched P/N/B-containing oligomer as multifunctional flame retar dant for epoxy resins[J]. Compos Part B, 2022, 234: 109701.
[25] CAI H P, HUANG W Y, LI B L, et al. A multi-element flame retardant for rail transit to improve the flame ret ardant performance of epoxy resin while reducing smoke density[J]. J Appl Polym Sci, 2022, 141(4): e5484 1.
[26] LU J Y, CHEN L P, LUO Z L, et al. A vanillin-containing DOPO-based compound for improving the flame reta rdancy of epoxy resin simultaneously with comparable transparency and mechanical property[J]. J Appl P olym Sci, 2021, 140(9): e53556.
[27] KIM H H, SIM M J, LEE J C, et al. The effects of chemical structure for phosphorus-nitrogen flame retardan ts on flame retardant mechanisms[J]. J Mater Sci, 2021, 58: 6850-6864.
[28] WAN C, DUAN H J, ZHANG C H, et al. A P/N/S-containing compound toward enhanced fire safety epoxy re sin with well-balanced performance[J]. Polym Degrad Stab, 2021, 192: 109698.
[29] YANG X Y, SHI J J, ZHOU Y J, et al. Enhanced flame retardancy of epoxy resins by intercalation of magnesiu m-aluminum hydrotalcite with phosphorus-based flame retardants[J]. Chin J Appl Chem, 2022, 41(8): 115 4-1167.
[30] WEI Z B, CHEN X L, JIAO C M. Thermal degradation and flame retardancy of fumaric acid in thermoplastic polyurethane elastomer[J]. Polym Adv Technol, 2019, 30(2): 475-482.
[31] HUANG G B, CHEN W, WU T, et al. Multifunctional graphene-based nano-additives toward high-performa nce polymer nanocomposites with enhanced mechanical, thermal, flame retardancy and smoke suppressi ve properties[J]. Chem Eng J, 2021, 410: 127590.
[32] LIU C, WU W, SHI Y Q, et al. Creating MXene/reduced graphene oxide hybrid towards highly fire safe ther moplastic polyurethane nanocomposites[J]. Compos Part B, 2020, 203: 108486.
[33] LIU Y, ZHAO J, DENG C L, et al. Flame-retardant effect of sepiolite on an intumescent flame-retardant poly propylene system[J]. Ind Eng Chem Res, 2011, 50(4): 2047-2054.
[34] LI W J, LUO F B, DAI Y M, et al. Fabrication of highly efficient flame-retardant and biocompatible ramie fab rics through covalent bonding and layer-by-layer assembly methods[J]. Cellulose, 2022, 31(14): 9025-904 2.
[35] ZOU Y B, CUI W Q, CHEN D L, et al. In situ-generated heat-resistant hydrogen-bonded organic framework for remarkably improving both flame retardancy and mechanical properties of epoxy composites[J]. ACS Appl Mater Interfaces, 2021, 15(40): 47463-47474.
[36] WANG X, WU T, HONG J, et al. Organophosphorus modified hollow bimetallic organic frameworks: effecti ve adsorption and catalytic charring of pyrolytic volatiles[J]. Chem Eng J, 2021, 421: 129697.